A Prospective Evaluation of ^{18}F-FDG and ^{11}C-Acetate PET/CT for Detection of Primary and Metastatic Hepatocellular Carcinoma

Joong-Won Park[1], Ji Hoon Kim[1], Seok Ki Kim[2], Keon Wook Kang[2], Kyung Woo Park[3], Jun-Il Choi[1], Woo Jin Lee[1], Chang-Min Kim[1], and Byung Ho Nam[4]

[1]Center for Liver Cancer, National Cancer Center, Goyang, Gyeonggi-do, Republic of Korea; [2]Department of Nuclear Medicine, National Cancer Center, Goyang, Gyeonggi-do, Republic of Korea; [3]Center for Cancer Prevention and Detection, National Cancer Center, Goyang, Gyeonggi-do, Republic of Korea; and [4]Cancer Registration and Biostatistics Branch, National Cancer Center, Goyang, Gyeonggi-do, Republic of Korea

Because ^{18}F-FDG PET has insufficient sensitivity for the detection of hepatocellular carcinoma (HCC), ^{11}C-acetate PET has been proposed as another technique for this use. We prospectively evaluated the value of PET/CT using these 2 tracers for the detection of primary and metastatic HCC. **Methods:** One hundred twelve patients (99 with HCC, 13 with cholangiocellular carcinoma) underwent biopsy and ^{18}F-FDG and ^{11}C-acetate PET/CT. **Results:** The overall sensitivities of ^{18}F-FDG, ^{11}C-acetate, and dual-tracer PET/CT in the detection of 110 lesions in 90 patients with primary HCC were 60.9%, 75.4%, and 82.7%, respectively. Elevated serum α-fetoprotein levels, an advanced tumor stage, portal vein tumor thrombosis, large tumors, and multiple tumors were significantly associated with positive ^{18}F-FDG PET/CT results. Uptake of ^{11}C-acetate was associated with large and multiple tumors. For ^{18}F-FDG, the sensitivities according to tumor size (1–2, 2–5, and ≥5 cm) were 27.2%, 47.8%, and 92.8%, respectively; for ^{11}C-acetate, these respective values were 31.8%, 78.2%, and 95.2%. ^{18}F-FDG was more sensitive in the detection of poorly differentiated HCC. Overall survival was lower in patients with ^{18}F-FDG PET/CT positive for all indexed lesions than in those with FDG negative or partially positive through the entire follow-up period. In analysis based on biopsied lesions, the sensitivity of ^{18}F-FDG PET/CT was 64.4% for primary HCC and 84.4% for ^{11}C-acetate PET/CT. The overall sensitivities of ^{18}F-FDG, ^{11}C-acetate, and dual-tracer PET/CT for 35 metastatic HCCs were 85.7%, 77.0%, and 85.7%, respectively. There was no significant difference in the sensitivity of tracers according to metastatic tumor size, location, or differentiation. **Conclusion:** The addition of ^{11}C-acetate to ^{18}F-FDG PET/CT increases the overall sensitivity for the detection of primary HCC but not for the detection of extrahepatic metastases. ^{18}F-FDG, ^{11}C-acetate, and dual-tracer PET/CT have a low sensitivity for the detection of small primary HCC, but ^{18}F-FDG PET/CT has a relatively high sensitivity for the detection of extrahepatic metastases of HCC.

Received Jun. 10, 2008; revision accepted Aug. 22, 2008.

For correspondence or reprints contact: Joong-Won Park, Center for Liver Cancer, National Cancer Center, 809 Madu-dong, Ilsan-gu, Goyang, Gyeonggi-do, 411-769, Republic of Korea.

E-mail: jwpark@ncc.re.kr

Key Words: hepatology; oncology; PET/CT; FDG; acetate; hepatocellular carcinoma; sensitivity

J Nucl Med 2008; 49:1912–1921
DOI: 10.2967/jnumed.108.055087

The prognosis of patients with hepatocellular carcinoma (HCC) is related to tumor stage at presentation and underlying liver function. Reliable staging of HCC is a fundamental precondition for deciding on the treatment modality, and the Barcelona Clinic Liver Cancer (BCLC) staging system links tumor stage with treatment modality (*1*). In particular, accurate characterization of primary and metastatic HCC, showing the tendency toward early vascular invasion of the tumor (*2*), is critical for proper treatment (*2*). Imaging studies by dynamic CT and contrast-enhanced MRI are important in the diagnosis and staging of HCC (*1,3,4*), but there is no consensus on which imaging tests are proper for detecting extrahepatic metastases. Whole-body PET has been used in a portion of HCC patients, but its usefulness has not yet been established.

Because whole-body combined PET/CT using ^{18}F-FDG effectively detects numerous cancerous lesions (*5*), this method was expected to improve the accuracy of HCC staging. However, the high level of glucose-6-phosphatase in liver tissue leads to the release of FDG-6-phosphate, resulting in reduced accumulation in differentiated HCCs (*6*). Thus, ^{18}F-FDG PET has an average false-negative rate of 40%−50% for the detection of HCC (*7*), and data on the role of PET/CT in the detection of HCC metastasis are limited (*7–9*).

^{11}C-labeled acetate PET effectively detects urologic malignancies (*10*). This tracer enters the Krebs cycle as a substrate for β-oxidation in fatty acid synthesis and cholesterol synthesis. Fatty acid synthesis is believed to be the major reason for uptake of ^{11}C-acetate by liver tumors. Recently, a Chinese study reported that ^{11}C-acetate PET

has improved sensitivity for detection of well-differentiated HCCs and that none of the primary HCC lesions was negative for ^{18}F-FDG and ^{11}C-acetate tracers (*6*). However, that study did not analyze sensitivity with regard to clinical and tumor characteristics, including underlying liver function and tumor stage. PET/CT is used mainly to screen for tumor metastasis, and its use is increasing because of an increasing number of candidates for curative treatment such as liver transplantation. Previous studies of PET/CT in patients with primary and metastatic HCC enrolled few patients or were retrospective (*7–9,11,12*).

The aim of this prospective study was to validate the value of ^{18}F-FDG and ^{11}C-acetate PET/CT for the detection of primary and metastatic HCC in 112 patients admitted to our center for diagnosis and treatment of primary liver cancer.

MATERIALS AND METHODS

Patients

Between June 2006 and April 2007, 112 patients diagnosed with primary liver cancer at the National Cancer Center Hospital (Goyang, South Korea) were prospectively enrolled. All patients gave informed consent, and the study was approved by the Internal Review Board at the hospital. All patients had newly diagnosed HCC, cholangiocellular carcinoma (CCC), or a newly diagnosed distant metastasis after curative resection of HCC that was performed 6 mo before this study. Patients underwent ^{18}F-FDG and ^{11}C-acetate PET/CT free of charge before treatment. Clinical diagnosis of primary HCC was based on the guidelines of the Korean Liver Cancer Study Group and the National Cancer Center of Korea (*13*). CCC was diagnosed by pathologic examination and exclusion of other metastatic adenocarcinomas. All 112 patients were examined by spiral CT, and imaging was confirmed pathologically by liver biopsy or operative tumor resection that was performed 1 wk before or after PET/CT. Liver biopsy was performed on a typical index lesion. The inclusion criteria of subjects were as follows: age between 18 and 80 y, Eastern Cooperative Oncology Group performance status of 0–2, adequate liver function (Child–Pugh classification A or B), and adequate renal function (serum creatinine $<$ 1.4 mg/dL). Patients were excluded if they had any other malignancy, a concurrent nonmalignant severe illness, or a psychiatric disorder.

Metastatic HCC lesions were screened and followed by chest radiography and routine spiral liver CT that covered the area from the hila of the lungs through the symphysis pubis or (in the case of suspected positive symptoms) by additional bone scanning and brain MRI. HCC metastasis was confirmed by histopathologic diagnosis (in the case of tumor resection or biopsy), by follow-up chest spiral CT with compatible nodules (when there was no clinical evidence of a benign tumor or inflammation), or by bone MRI or bone CT. Intraabdominal metastases and brain metastases were diagnosed by routine spiral liver CT and brain MRI. An intraabdominal lymph node metastasis was considered to be present when the node was more than 1 cm in diameter.

The absence of HCC metastasis was confirmed by the serum level of α-fetoprotein and by imaging (chest radiography and routine spiral liver CT covering the area from the hila of the lungs through the symphysis pubis) performed at the 3-mo follow-up.

Imaging Studies and Biopsy

Routine spiral CT was performed with multidetector CT scanners (Lightspeed pro-16; GE Healthcare). Images were acquired in a craniocaudal direction from the hila of the lungs through the symphysis pubis with 1.25 × 16 mm beam collimation and a reconstruction interval of 3.0 mm. Hepatic artery–phase imaging was initiated 25 s after contrast medium injection. After administration of the contrast medium, the portal vein phase and equilibrium phase were acquired at 70 and 180 s, respectively.

MRI was performed on a 1.5-T superconducting scanner (Sigma; GE Healthcare) with a torso coil for signal reception. Baseline MRI was performed, and dynamic imaging was performed before and after administration of gadopentetate dimeglumine (Magnevist; Schering). Superparamagnetic iron oxide–enhanced MRI was performed immediately after gadolinium-enhanced dynamic MRI. For superparamagnetic iron oxide–enhanced MRI, ferumoxides (Feridex I.V.; Advanced Magnetics) were administered and images were obtained at 30 s (hepatic artery phase), 70 s (portal vein phase), and 3–5 min (delayed phase). Spiral CT and contrast-enhanced MRI were evaluated by 2 expert radiologists.

Sonographically guided percutaneous core biopsies were performed using a freehand technique. All biopsies were performed with a 3.5- to 5-MHz convex probe (Acuson Sequia 512; Siemens Medical Solutions) with 18-gauge automated core biopsy needles (Acecut; TSK). Specimens were routinely processed and were stained with hematoxylin and eosin and by the Masson trichrome method. HCC was diagnosed according to the criteria of the International Working Party (*14*).

^{18}F-FDG and ^{11}C-Acetate PET/CT

^{11}C-acetate was synthesized using a fully automated custom-made radiochemistry module based on the solid-phase extraction method of Roeda et al. (*15*). ^{18}F-FDG was synthesized at our hospital using an automated radiochemistry module (Chemical Process Control Unit; CTI/Siemens).

PET studies were performed with a dedicated PET scanner (Biograph LSO; Siemens Medical Systems) or a PET/CT scanner (Discovery LS; GE Healthcare). For the Biograph LSO scanner, we used a scout view with 30 mA and 130 kVp, followed by a spiral CT scan with an effective milliamperage of 50, 130 kVp, a 5-mm section width, a 4-mm collimation, a 12-mm table feed per rotation, 0.8 s per rotation, and the patient's arms raised. For the Discovery LS scanner, we used a scout view with 30 mA and 120 kVp, followed by a spiral CT scan with a 0.8-s rotation time, 80 mA, 140 kVp, a 5-mm section thickness, a 4.25-mm interval in high-speed mode, and the patient's arms at the sides of the torso. PET images were acquired after CT scans at 3 min per bed position of 11.2 cm in the 3-dimensional acquisition mode (Biograph LSO) or 4 min per bed position of 14.2 cm in the 2-dimensional acquisition mode (Discovery LS). CT images were reconstructed onto a 512 × 512 matrix and converted into 511-keV-equivalent attenuation factors for attenuation correction. PET images were reconstructed onto a 128 × 128 matrix using ordered-subsets expectation maximization and attenuation correction. The standardized uptake value (SUV) was calculated as (decay-corrected activity [kBq] per milliliter of tissue volume)/(injected ^{18}F-FDG activity [kBq]/body mass [g]). The SUVs of lesions were obtained by placing regions of interest manually around the lesion. The maximum SUV within a region of interest was used to minimize partial-volume effects.

All patients were normoglycemic and had fasted, except for water and medications, for at least 8 h before the PET studies. ^{11}C-acetate PET/CT was performed first, and ^{18}F-FDG PET/CT was performed at least 4 h later.

^{11}C-Acetate PET/CT. Whole-body static PET/CT scans, obtained 20 min after intravenous injection of about 370–555 MBq (10–15 mCi) of ^{11}C-acetate, were acquired from the cerebellum to the upper third of the femur with 6–7 frames. To enhance and standardize tumor uptake of ^{18}F-FDG, we had the patients continue to fast after ^{11}C-acetate PET/CT until the end of the ^{18}F-FDG PET/CT study.

^{18}F-FDG PET/CT. The patients were kept well hydrated because ^{18}F-FDG is excreted through the kidney and urinary bladder. Twenty milligrams of furosemide were administered intravenously within 10 min of the ^{18}F-FDG injection, and then 500 mL of water were given. ^{18}F-FDG (444–740 MBq [12–20 mCi]) was injected intravenously 4 h after ^{11}C-acetate PET/CT. Patients were encouraged to rest during the ^{18}F-FDG uptake period. Sixty minutes after ^{18}F-FDG injection, whole-body static PET/CT was performed using the same method as for whole-body ^{11}C-acetate PET/CT.

PET/CT Analysis

Separate CT and PET scan data were accurately coregistered. PET, PET/CT, and CT images were reviewed using a dedicated workstation and software (eNtegra; GE Healthcare, and e.Soft; Siemens Medical Solutions). With this system, 3-dimensional displays (transaxial, coronal, and sagittal) were available, as were maximum-intensity projections of the PET data. PET/CT scans were interpreted by 2 nuclear medicine physicians, who were unaware of the results of other imaging studies on these patients. Intrahepatic primary lesions were interpreted visually using a 3-point grading system (isometabolic, hypermetabolic, and hypometabolic) that compared data with tracer uptake by normal liver parenchyma for ^{11}C-acetate and ^{18}F-FDG PET. If a lesion was hypermetabolic on at least 1 image from ^{11}C-acetate or ^{18}F-FDG PET, it was assumed to be a malignant hepatic mass. Extrahepatic lesions were interpreted visually using a 5-point scale: 0, no visible accumulation; 1, less accumulation than in the liver; 2, accumulation about the same as in the liver; 3, more accumulation than in the liver but less than in the brain cortex; 4, accumulation comparable to that of the brain cortex (*16*). An extrahepatic lesion was considered to be malignant when its accumulation of ^{18}F-FDG or ^{11}C-acetate was over 3 on this scale.

Interpretation and Statistical Analysis

To assess the diagnostic accuracy of ^{18}F-FDG and ^{11}C-acetate PET/CT, we calculated values in a lesion-to-lesion analysis for all primary liver cancer lesions, lymph nodes, and distant metastases. All analyzed lesions were larger than 1 cm and were interpreted according to the criteria described above for spiral CT or contrast-enhanced MRI. Patient-based analysis was also performed. For the subgroup of patients with more than 4 lesions or with diffuse infiltrative tumors, the index lesion was assigned as the representative lesion or area before PET/CT analysis. Liver biopsy sites were identified if biopsies were performed before PET/CT analysis.

The data were analyzed using STATA software, version 9.1 (StataCorp LP). The Pearson χ^2 test and Fisher exact test were used for categoric variables, and the Student t test was used for continuous variables. The results of all continuous variables are expressed as the mean ± SD. The Kaplan–Meier method was used to estimate overall survival curves, and survival curves were compared using the log-rank test. Results were considered significant if the P value was less than 0.05.

RESULTS

Patient Characteristics

The characteristics of the 112 patients (99 with HCC, 13 with CCC) are summarized in Table 1. The mean age was 57.6 ± 10.4 y (range, 34–85 y), and the sex ratio (M:F) was 3.7:1. Eighty-three patients (74.1%) tested positive for the hepatitis B surface antigen. Ten patients had hepatitis C, 10 had a history of alcohol abuse, and 10 had non-B/non-C/nonalcoholic etiologies. One hundred one patients had a Child–Pugh classification of A. Nine patients who underwent surgical resection had distant metastases but no primary liver lesions; hence we analyzed 90 patients for primary tumor characteristics. Analysis of the maximal diameter of tumors showed that 7 patients (7.8%) had lesions 1–2 cm in diameter, 42 patients (46.7%) had lesions 2–5 cm in diameter, and 41 patients (45.5%) had lesions 5 cm or more in diameter. Analysis of the number of nodules showed that 46 patients (51.1%) had 1 nodule, 11 patients (12.2%) had 2 nodules, 3 patients (3.3%) had 3 nodules, and 30 patients (33.3%) had more than 3 nodules. Of the 99 HCC patients, 7 had biopsy specimens that were inadequate for evaluation of tumor differentiation. We evaluated the other 92 patients (83 with primary HCC, 9 with metastatic HCC) using the Edmonson–Steiner grading system. Nine patients were grade I, 51 were grade II, 29 were grade III, and 3 were grade IV. Serum α-fetoprotein levels less than 20 ng/mL were detected in 43 HCC patients (43.4%). Using the modified Union Internationale Contre le Cancer (International Union Against Cancer) (UICC) staging system, we enrolled 5 (5.1%) stage I patients, 37 (37.3%) stage II patients, 16 (16.2%) stage III patients, 13 (13.1%) stage IVa patients, and 28 (28.3%) stage IVb patients. According to the BCLC staging system, 21 patients (21.4%) were in very early or early stage HCC, 35 patients (35.7%) were in intermediate stage HCC, and 43 patients (44%) in advanced or terminal stage HCC (Table 1).

Lesion Uptake of PET/CT: Patient-Based Analysis

Among the 99 HCC patients, we evaluated all positive results from ^{18}F-FDG and ^{11}C-acetate PET/CT (Tables 2 and 3; Fig. 1). Because the number of index lesions varied from 1 to 4 in each patient, we classified analysis of PET positives in all lesions and partial lesions. In our patient-based analysis, a PET-positive result indicates a positive result for all index lesions. The following factors were significantly associated with uptake of ^{18}F-FDG findings on PET/CT: level of serum α-fetoprotein, modified UICC stage, BCLC stage, tumor size, number of tumors, and presence of portal vein invasion. Higher levels of serum α-fetoprotein

TABLE 1
Baseline Characteristics

Characteristic	HCC, $n = 99$	CCC, $n = 13$
Age (y)		
<50	29 (29.3)	1 (7.7)
≥50	70 (70.7)	12 (92.3)
Sex		
Male	78 (78.8)	10 (76.9)
Female	21 (21.2)	3 (23.1)
Etiology*		
Hepatitis B	79 (79.8)	4 (30.8)
Hepatitis C	8 (8.1)	2 (15.4)
Alcohol	8 (8.1)	2 (15.4)
Other	5 (5.0)	5 (38.4)
Child–Pugh class		
A	89 (89.9)	12 (92.3)
B	10 (10.1)	1 (7.7)
EGOG performance		
0	65 (65.7)	8 (61.5)
1	27 (27.2)	3 (23.1)
2	7 (7.1)	2 (15.4)
Tumor size† (cm)		
≥1, <2	7 (7.8)	0 (0)
≥2, <5	42 (46.7)	4 (30.8)
≥5	41 (45.5)	9 (69.2)
Tumor number†		
1	46 (51.1)	5 (38.5)
2	11 (12.2)	0 (0)
3	3 (3.3)	0 (0)
≥4	30 (33.4)	8 (61.5)
Tumor type†		
Well defined	78 (86.7)	6 (46.2)
Ill defined	12 (13.3)	7 (53.8)
Portal/hepatic vein invasion†		
No	63 (70.0)	7 (53.8)
Yes	27 (30.0)	6 (46.2)
Tumor differentiation‡		
I	9 (9.8)	—
II	51 (55.4)	—
III	29 (31.6)	—
IV	3 (3.3)	—
α-fetoprotein (ng/mL)		
<20	43 (43.4)	—
20–400	28 (28.3)	—
>400	28 (28.3)	—
Modified UICC stage		
I	5 (5.1)	0 (0)
II	37 (37.3)	3 (23.1)
III	16 (16.2)	3 (23.1)
IVa	13 (13.1)	3 (23.1)
IVb	28 (28.3)	4 (30.7)
BCLC stage		
Very early	5 (5.1)	—
Early	16 (16.3)	—
Intermediate	35 (35.7)	—
Advanced	42 (42.9)	—
Terminal	1 (1.0)	—

*One patient had both hepatitis B virus and hepatitis C virus.

†Among 99 HCC patients, 9 patients had only distant metastases without primary liver lesion after previous resection and 90 patients had primary HCC.

‡Edmonson–Steiner grade: 7 of 90 patients with primary HCC had inappropriate biopsy specimen for evaluation of pathologic grade, and 92 patients (83 primary HCC and 9 metastatic HCC) were finally evaluated.

ECOG = Eastern Cooperative Oncology Group.

Data in parentheses are percentages.

and larger tumors were associated with positive ^{18}F-FDG PET/CT results ($P < 0.001$). None of the 7 patients with small tumors (<2 cm in diameter), 18 of 42 patients (43%) with tumors 2–5 cm in diameter, and 32 of 41 patients (78%) with tumors larger than 5 cm had positive findings for all index lesions on ^{18}F-FDG PET/CT. However, the differences between these groups were not statistically significant (Table 3). None of the patients in modified UICC stage I and none of the patients in the very early BCLC stage had positive findings on ^{18}F-FDG PET/CT. In contrast, 11 of 13 patients (85%) in modified UICC stage IVa and 31 of 42 patients (74%) in the advanced BCLC stage had positive findings on ^{18}F-FDG PET/CT. Figure 2 shows the association between ^{18}F-FDG PET/CT and overall survival in HCC patients. Patients with positive ^{18}F-FDG PET/CT findings for all indexed lesions had significantly lower survival than did patients with negative or partially positive ^{18}F-FDG PET/CT findings ($P = 0.0421$).

The significant factors for uptake of ^{11}C-acetate were tumor size and number of tumors (Tables 2 and 3). Any clinical factors and staging were not associated with uptake of ^{11}C-acetate PET/CT. In contrast to our ^{18}F-FDG PET/CT results, in 2 of 5 patients (40%) in modified UICC stage I and 31 of 37 patients (84%) in modified UICC stage II, all lesions were positive on ^{11}C-acetate PET/CT. In 2 of 7 patients (29%) with small tumors (diameter < 2 cm) and 29 of 42 patients (69%) with 2- to 5-cm tumors, all lesions were positive on ^{11}C-acetate PET/CT ($P = 0.003$; Table 3). Compared with ^{18}F-FDG PET/CT, ^{11}C-acetate PET/CT showed positive findings for all lesions in more patients with the following characteristics: the male sex, a performance status of 0, a serum α-fetoprotein level of less than 20 ng/mL, hepatitis B virus positive, modified UICC stage II, an intermediate-sized (2–5 cm) tumor, a single tumor, a well-defined tumor, and no portal vein invasion ($P < 0.05$). The positivity of ^{11}C-acetate PET/CT was not related to the survival of HCC patients ($P = 0.7271$).

Sensitivity for Detection of Primary Liver Cancer by PET/CT: Lesion-Based Analysis

Among the 110 lesions of the 90 patients with primary HCC, we evaluated the lesions that were positive on ^{18}F-FDG and ^{11}C-acetate PET/CT (Table 4; Fig. 3). Tumor size, number of tumors, and tumor differentiation were significantly associated with the sensitivity for detection of primary HCC on ^{18}F-FDG PET/CT ($P < 0.05$). The sensitivity for detection of HCC by ^{18}F-FDG PET/CT was 27.2%, 47.8%, and 92.8% in index lesions sized 1–2 cm, 2–5 cm, and 5 cm or more, respectively. Twenty-seven of 46 single lesions (58.8%) and 26 of 33 index lesions (79%) in patients who had more than 3 lesions were positive on ^{18}F-FDG PET/CT. ^{18}F-FDG PET/CT had significantly higher sensitivity for poorly differentiated HCC (Edmonson–Steiner grades III and IV) than for well-differentiated HCC (grades I and II; $P < 0.001$).

TABLE 2
Lesion Uptake of ^{18}F-FDG and ^{11}C-Acetate on PET/CT: Patient-Based Analysis of 99 Patients with Primary and Metastatic HCC

Characteristic	No. of patients (n = 99)	^{18}F-FDG		^{11}C-acetate		P* between 2 PET/CT types
		Patients with all lesions positive (n)	P	Patients with all lesions positive (n)	P	
Age (y)						
<50	29	18 (62)	NS	23 (79)	NS	NS
≥50	70	40 (57)		46 (66)		NS
Sex						
Male	78	44 (56)	NS	56 (72)	NS	0.008
Female	21	14 (67)		13 (62)		NS
ECOG performance						
0	65	33 (51)	NS	45 (69)	NS	0.008
1	27	21 (78)		19 (70)		NS
2	7	4 (57)		5 (71)		NS
Child–Pugh class						
A	89	52 (58)	NS	63 (71)	NS	0.016
B	10	6 (60)		6 (60)		NS
Etiology†						
Hepatitis B virus	79	46 (58)	NS	55 (70)	NS	0.039
Hepatitis C virus	8	6 (75)		6 (75)		NS
Alcohol	8	4 (50)		5 (63)		NS
Other	5	3 (60)		4 (80)		NS
α-fetoprotein (ng/mL)						
<20	43	19 (44)	0.002	29 (67)	NS	0.006
20–400	28	15 (54)		19 (68)		NS
>400	28	24 (86)		21 (75)		NS
Modified UICC stage						
I	5	0 (0)	0.002	2 (40)	NS	NS
II	37	23 (62)		31 (84)		0.022
III	16	5 (31)		9 (56)		NS
IVa	13	11 (85)		9 (69)		NS
IVb	28	19 (68)		18 (64)		NS
BCLC stage						
Very early	5	0 (0)	<0.001	2 (40)	NS	NS
Early	16	4 (25)		10 (63)		NS
Intermediate	35	23 (66)		28 (80)		NS
Advanced	42	31 (74)		28 (67)		NS
Terminal	1	0 (0)		1 (100)		—

*Comparison of positives between ^{18}F-FDG and ^{11}C-acetate PET/CT according to clinical characteristics using McNemar χ^2 test.
†One patient had both hepatitis B virus and hepatitis C virus.
NS = not significant; ECOG = Eastern Cooperative Oncology Group.
Data in parentheses are percentages.

The sensitivity of ^{11}C-acetate PET/CT for the detection of primary HCC was significantly associated with tumor size and number of tumors (Table 4). The sensitivity for detection of primary HCC on ^{11}C-acetate PET/CT was 31.8%, 78.2%, and 95.2% in index lesions sized 1–2 cm, 2–5 cm, and 5 cm or more, respectively. Larger tumors were associated with significantly greater sensitivity ($P <$ 0.001). Thirty-seven of 46 single lesions (80.4%) and 28 of 33 index lesions in patients with multiple lesions (84.8%) were positive for ^{11}C-acetate uptake on PET/CT. Comparison of the 2 PET modalities indicates that ^{11}C-acetate PET/CT had significantly higher sensitivity for detection of medium-sized tumors (2–5 cm), single tumors, and well-differentiated tumors ($P < 0.05$). The statistics for the maximum SUV of the 110 index lesions are summarized in Table 5.

For detection of the 110 index lesions in patients with primary HCC, the sensitivity of ^{18}F-FDG PET/CT was 60.9%, the sensitivity of ^{11}C-acetate PET/CT was 75.4%, and the sensitivity of dual tracers was 82.7%. Among the 90 HCC lesions that underwent biopsy, ^{18}F-FDG PET/CT detected 58 lesions (a sensitivity of 64.4%) and ^{11}C-acetate PET/CT detected 76 lesions (a sensitivity of 84.4%). Of the 13 CCC lesions that underwent biopsy, all were positive by ^{18}F-FDG PET/CT (a sensitivity of 100%) and 9 were positive by ^{11}C-acetate PET/CT (a sensitivity of 69.2%).

TABLE 3
Lesion Uptake of ^{18}F-FDG and ^{11}C-Acetate on PET/CT: Patient-Based Analysis of 90 Patients with Primary HCC

Characteristic	No. of patients (n = 90)	^{18}F-FDG Patients with all lesions positive (n)	^{18}F-FDG P	^{11}C-acetate Patients with all lesions positive (n)	^{11}C-acetate P	P* between 2 PET/CT types
Tumor size (cm)						
≥1, <2	7	0 (0)	<0.001	2 (29)	0.030	NS
≥2, <5	42	18 (43)		29 (69)		0.003
≥5	41	32 (78)		32 (78)		NS
			<0.001†		0.023†	
Tumor number						
1	46	26 (57)	0.001	36 (78)	0.001	0.006
2–3	14	2 (14)		4 (29)		NS
≥4	30	22 (73)		23 (77)		NS
			NS†		NS†	
Tumor type						
Well defined	78	42 (54)	NS	55 (71)	NS	0.002
Ill defined	12	8 (67)		8 (67)		NS
Portal vein invasion						
No	63	29 (46)	0.005	43 (68)	NS	0.001
Yes	27	21 (78)		20 (70)		NS

*Comparison of positives between ^{18}F-FDG and ^{11}C-acetate PET/CT according to tumor characteristics using McNemar χ^2 test.
†Score test for trend.
NS = not significant.
Data in parentheses are percentages.

Sensitivity for Detection of Metastatic HCC by PET/CT

For the 28 patients with modified UICC stage IVb HCC, patient-based analysis indicated that 19 (68%) were positive for ^{18}F-FDG and 18 (64%) were positive for ^{11}C-acetate. In this analysis, "positive" indicated positive for all index lesions and metastases in each patient (Table 2).

For lesion-based analysis, we evaluated the sensitivity of PET/CT in the detection of 35 metastatic HCC index lesions in 28 patients (Table 6). The locations of distant metastases were lung (20 lesions), bone (6 lesions), adrenal gland (4 lesions), abdominal peritoneum (3 lesions), brain (1 lesion), and left atrium of the heart (1 lesion). The overall sensitivity of ^{18}F-FDG and ^{11}C-acetate PET/CT in

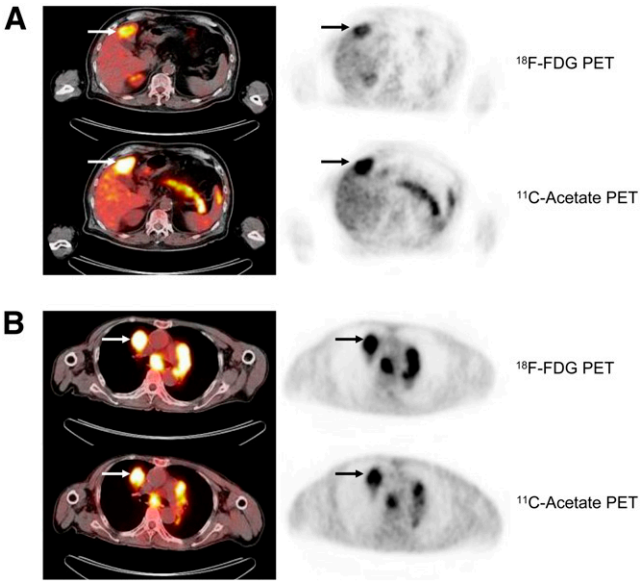

FIGURE 1. Detection of HCC with ^{18}F-FDG PET/CT and ^{11}C-acetate PET/CT on transaxial sections of liver and chest. Panels on left show PET/CT, and panels on right show PET. (A) Primary HCC of liver was markedly positive for uptake with both tracers (arrows). (B) Metastatic HCC of upper lobe of right lung was markedly positive for uptake with both tracers (arrows).

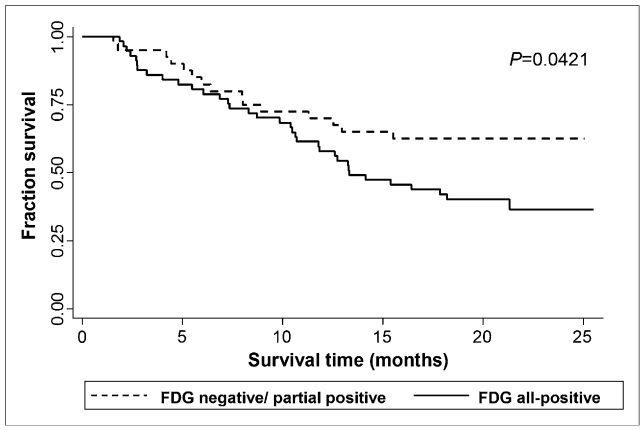

FIGURE 2. Overall survival after diagnosis of HCC. Kaplan–Meier survival plots are classified by positivity of ^{18}F-FDG. Overall survival was lower in patients with positive ^{18}F-FDG findings than in those with negative or partially positive ^{18}F-FDG findings through entire follow-up period. P values were calculated using log-rank test.

TABLE 4
Sensitivity of ^{18}F-FDG and ^{11}C-Acetate PET/CT in 90 Patients with Primary HCC: Lesion-Based Analysis of 110 Lesions

Characteristic	No. of index lesion (n = 110)	^{18}F-FDG Lesions positive (n)	^{18}F-FDG P	^{11}C-acetate Lesions positive (n)	^{11}C-acetate P	P* between 2 PET/CT types
Tumor size (cm)						
≥1, <2	22	6 (27.2)	<0.001	7 (31.8)	<0.001	NS
≥2, <5	46	22 (47.8)		36 (78.2)		0.001
≥5	42	39 (92.8)		40 (95.2)		NS
			<0.001†		<0.001†	
Tumor number						
1	46	27 (58.7)	0.021	37 (80.4)	0.027	0.006
2–3	31	14 (45.2)		18 (58.0)		NS
4	33	26 (78.8)		28 (84.8)		NS
			NS†		NS†	
Tumor differentiation‡						
I and II	70	35 (50.0)	<0.001	50 (71.4)	NS	0.006
III and IV	31	27 (87.0)		27 (90.0)		NS
			<0.001†		NS†	

*Comparison of sensitivity between ^{18}F-FDG and ^{11}C-acetate PET/CT according to tumor characteristics using McNemar χ^2 test.
†Score test for trend.
‡Edmonson–Steiner grade: 7 of 90 patients with primary HCC had inappropriate biopsy specimen for evaluation of pathologic grade, and 101 index lesions of 83 patients were finally evaluated.
NS = not significant.
Data in parentheses are sensitivity (%).

35 index lesions of 28 patients with metastatic HCC was 85.7%, 77.0%, and 85.7% by ^{18}F-FDG alone, ^{11}C-acetate alone, and both tracers, respectively. All positive lesions detected by ^{11}C-acetate (Fig. 4) were also positive on ^{18}F-FDG PET/CT. Additionally, 5 index lesions of the lymph node metastases 1 cm or larger were evaluated, 3 of which were positive on ^{18}F-FDG and ^{11}C-acetate PET/CT.

Of 20 small metastatic lesions (1–2 cm in diameter), 16 (80%) were detected on ^{18}F-FDG PET/CT and 13 (65%) on ^{11}C-acetate PET/CT. The sensitivity of both PET/CT tracers in the 15 metastatic lesions 2 cm or larger was the same: 93%. ^{18}F-FDG PET/CT detected 100% of HCC

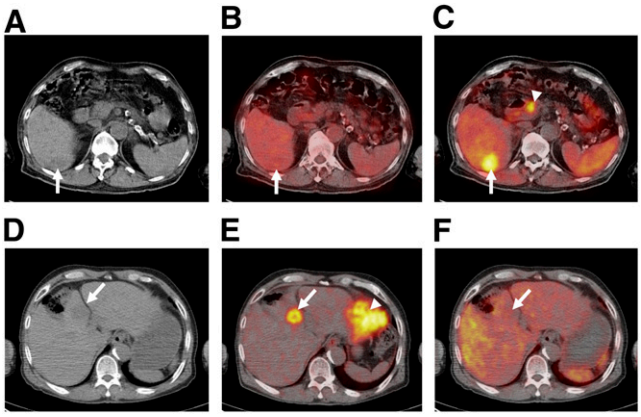

FIGURE 3. (A–C) Transaxial PET/CT images of 71-y-old man in whom HCC of Edmondson and Steiner's grade 1 was diagnosed. Unenhanced CT image shows hypoattenuating lesion in right lobe (arrow) (A), ^{18}F-FDG PET/CT image shows no focal ^{18}F-FDG accumulation in tumor (arrow) (B), and ^{11}C-acetate PET/CT image shows focally increased uptake of ^{11}C-acetate in tumor (arrow) and physiologic ^{11}C-acetate uptake in pancreas (arrowhead) (C). (D–F) Transaxial PET/CT images of 65-y-old man with HCC of Edmondson and Steiner's grade 3. Unenhanced CT image shows hypoattenuating lesion (arrow) (D), ^{18}F-FDG PET/CT image shows focal ^{18}F-FDG accumulation in tumor (arrow) and physiologic FDG uptake in myocardium (arrowhead) (E), and ^{11}C-acetate PET/CT image shows less intense accumulation in tumor (arrow) than in surrounding hepatic region (F).

TABLE 5
Maximum SUV of 110 Index Lesions Considered to Be Positive in 90 Patients with Primary HCC

Characteristic	No. of index lesions (n = 110)	^{18}F-FDG SUV	^{11}C-acetate SUV
Tumor size (cm)			
≥1, <2	22	4.54 ± 1.33	4.25 ± 2.10
≥2, <5	46	4.65 ± 1.06	5.53 ± 2.26
≥5	42	7.86 ± 5.24	4.86 ± 2.59
Tumor number			
1	46	4.95 ± 2.77	5.55 ± 2.52
2–3	31	7.76 ± 5.69	4.17 ± 1.88
≥4	33	7.46 ± 4.85	5.10 ± 2.50
Tumor differentiation*			
I and II	70	5.10 ± 2.67	5.27 ± 2.49
III and IV	31	7.66 ± 5.16	4.94 ± 2.18

*Edmonson–Steiner grade: 7 of 90 patients with primary HCC had inappropriate biopsy specimen for evaluation of pathologic grade, and 101 index lesions of 83 patients were finally evaluated.

TABLE 6
Sensitivity of ^{18}F-FDG and ^{11}C-Acetate PET/CT in 28 Patients with Metastatic HCC: Lesion-Based Analysis of 35 Index Lesions

Characteristic	No. of lesions (n = 35)	^{18}F-FDG		^{11}C-acetate		P* between 2 PET/CT types
		Lesions positive (n)	P	Lesions positive (n)	P	
Tumor size (cm)						
≥1, <2	20	16 (80)	NS	13 (65)	NS	NS
≥2	15	14 (93)		14 (93)		NS
			NS†		0.052†	
Metastasis location						
Lung	20	16 (80)	NS	14 (70)	NS	NS
Bone	6	6 (100)		6 (100)		
Adrenal gland	4	3 (75)		3 (75)		
Abdominal peritoneum	3	3 (100)		2 (66.7)		
Brain	1	1 (100)		1 (100)		
Left atrium of heart	1	1 (100)		1 (100)		
Tumor differentiation‡						
Grade I and II	22	20 (91)	NS	20 (91)	0.032	NS
Grade III and IV	13	10 (77)		7 (54)		NS
			NS†		0.013†	

*Comparison of positives between ^{18}F-FDG and ^{11}C-acetate PET/CT according to tumor characteristics using McNemar χ^2 test.
†Score test for trend.
‡Edmonson–Steiner grade.
NS = not significant.
Data in parentheses are sensitivity (%).

metastases in bone (6 cases) and the abdominal peritoneum (3 cases). ^{18}F-FDG PET/CT and ^{11}C-acetate PET/CT detected 80% and 70% of lung metastases, respectively. Tumor differentiation did not show any significant differences in positive findings between the 2 modalities (90% vs. 90.9% in grades I and II and 76.9% vs. 53.8% in grades III and IV). In a comparison with poorly differentiated HCC, metastatic tumors from well-differentiated HCC had a greater number of positive results with ^{11}C-acetate (P = 0.032). There was no significant difference between the 2 tracers in sensitivity for metastatic tumor size, location, or differentiation (Table 6).

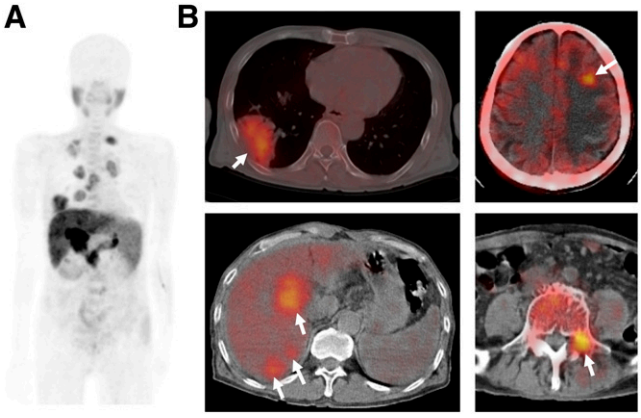

FIGURE 4. Transaxial PET/CT images of 63-y-old man in whom HCC of Edmondson and Steiner's grade 2 was diagnosed. ^{11}C-acetate PET maximal-intensity image (A) and integrated PET/CT images (B) show HCC in liver and multiple metastatic lesions (arrows) in brain, lung, and spine.

DISCUSSION

PET/CT is used in HCC patients to detect extrahepatic metastases (*11,17*), predict outcome after resection (*18,19*), select liver transplantation candidates (*20*), and assess residual tumors after treatment with transcatheter arterial chemoembolization or radiofrequency ablation (*21*). The usefulness of these applications depends on the ability of PET/CT to detect small or atypical lesions—those for which no diagnostic studies with spiral CT or contrast-enhanced MRI are available, those in the liver, and those in extrahepatic areas. Previous studies, which enrolled few patients or were retrospective, reported inadequate sensitivity for ^{18}F-FDG PET/CT in the detection of primary HCC (*22–26*) and suggested the addition of ^{11}C-acetate PET/CT to improve the accuracy of PET/CT (*6*). However, these studies did not provide sufficient clinical detail for hepatologists and oncologists, the primary users of PET/CT for liver tumors.

In this study, the overall sensitivity for the detection of primary HCC was 60.9% for ^{18}F-FDG alone, 75.4% for ^{11}C-acetate alone, and 82.7% for both tracers. Although dual-tracer PET/CT had better sensitivity, the results of tumor size–based analysis were disappointing. For 1- to 2-cm HCCs, the sensitivity was 27.2% with ^{18}F-FDG PET/

CT and 31.8% with ^{11}C-acetate PET/CT. Patient-based analysis indicated that none of the 5 patients with stage I HCC (modified UICC system) or very early stage HCC (BCLC system) had positive findings on ^{18}F-FDG PET/CT (Table 2). Therefore, ^{18}F-FDG and ^{11}C-acetate PET/CT appear not to be useful for the detection of small lesions in the liver. The morphologic distinction of small HCC tumors from other regenerative nodules and premalignant dysplastic nodules can be difficult. Several PET/CT studies have suggested that differentiation of these nodules is possible, but our results do not support this conclusion. Biopsy-based analysis indicated that the sensitivity was 64.4% by ^{18}F-FDG PET/CT and 84.4% by ^{11}C-acetate PET/CT, apparently better than the overall sensitivity. However, we cannot exclude selection bias such as selection of a larger tumor for biopsy as an indexed lesion. Comparison with other benign tumors is not reasonable in clinical settings, and we therefore designed this study for only HCC and CCC patients. This study design (99 HCC patients, 13 CCC patients), therefore, could be considered as a case-only design, allowing computation of only the test sensitivity. All 13 cases of CCC had positive findings on ^{18}F-FDG PET/CT. Although a previous study reported that ^{11}C-acetate did not accumulate in CCC (*6*), the number of patients in this study was only 3, and 9 of our 13 CCC patients had positive findings on ^{11}C-acetete PET/CT. Further study of the accuracy of ^{11}C-acetate PET/CT in CCC may be required.

We found that both tracers were more readily taken up when there were large tumors or a large number of tumors. Our patient-based analysis indicated that clinical factors (age, sex, etiology, performance, Child–Pugh class) did not affect tracer uptake. Serum α-fetoprotein level and tumor stage (by the modified UICC and the BCLC systems) affected uptake only of ^{18}F-FDG. For analyzing accuracy in the detection of small tumors or extrahepatic metastases, we prospectively enrolled more patients who had modified UICC stage I, II, and IVb, compared with the patient population of our previous report (*27*). A high rate of positive findings on ^{18}F-FDG PET has been reported in patients with elevated serum α-fetoprotein levels (*7*) and in patients with poorly differentiated HCC (*28*).

Our study also showed a high positive rate for both ^{18}F-FDG PET/CT and ^{11}C-acetate PET/CT in poorly differentiated HCC. ^{11}C-acetate accumulation was significantly better than ^{18}F-FDG accumulation in well-differentiated HCC (50% vs. 71.4%), but there was no difference between the tracers in poorly differentiated HCC (Table 4). These results differ from those of a previous report (*6*), possibly because we used a different protocol for classifying tumor differentiation (2 categories in this study). However, in comparing the 2 tracers, ^{11}C-acetate PET/CT yielded better results in male patients, in patients with better performance status, and in hepatitis B virus–positive patients. These results could be related to the biologic characteristics of the tumors and requires further study. A previous study reported that the 2-y recurrence-free survival rate of ^{18}F-FDG PET/CT–negative HCC patients was significantly higher than that of ^{18}F-FDG–positive HCC patients after liver transplantation (*20*). In this study, patients with positive ^{18}F-FDG PET/CT findings for all indexed lesions had a significantly lower survival rate (Fig. 2). Because uptake of ^{18}F-FDG PET/CT was associated with the level of serum α-fetoprotein, modified UICC stage, BCLC stage, tumor size, number of tumors, and presence or absence of portal vein invasion, multivariate analysis did not reveal positive ^{18}F-FDG findings to be an independent risk factor for survival.

^{18}F-FDG PET/CT might be useful in the evaluation of extrahepatic metastases, although data supporting this possibility are limited (*7–9,11,12*). To our knowledge, our study is the first that has prospectively evaluated the sensitivity of dual-tracer PET/CT for the detection of HCC metastases. Our patient-based analysis indicated that only 68% of stage IVb HCC patients (modified UICC system) had positive ^{18}F-FDG findings for all lesions, including primary and metastatic HCC (Table 2). The finding of no ^{18}F-FDG uptake by primary HCC lesions decreased the positive rate in this patient-based analysis. However, our lesion-based analysis of 35 indexed extrahepatic metastases indicated that ^{18}F-FDG PET/CT detected 80% of lung metastases and 100% of bone metastases (Table 6). Lung and bone are the 2 major sites of HCC metastases. A metastatic tumor diameter greater than 1 cm had no effect on the sensitivity of detection by either tracer, and well-differentiated tumors were more likely to test positive with ^{11}C-acetate. In contrast to detection of primary 1- to 2-cm HCCs, ^{18}F-FDG PET/CT was more sensitive than ^{11}C-acetate PET/CT for detecting metastases, although this difference was not statistically significant (Table 6). For metastatic HCC, dual-tracer PET/CT was not superior to ^{18}F-FDG alone. A previous comparison of bone scintigraphy and ^{18}F-FDG PET/CT reported that PET/CT was more sensitive, but that study provided no data about HCC (*29*). Evaluating the usefulness of ^{18}F-FDG PET/CT for screening extrahepatic HCC metastases requires a further cost–benefit study.

Our study had some limitations. Histopathologic confirmation of metastases (the gold standard) was not possible in all cases. In our prospective study, we screened for metastatic HCC lesions and followed up with imaging studies or additional methods. The absence of HCC metastasis was confirmed by the level of serum α-fetoprotein and by imaging (chest radiography and routine spiral liver CT covering from the hila of the lungs through the symphysis pubis) performed at the 3-mo follow-up. The criteria we used to determine metastasis may have resulted in some underestimation, even though the study was prospective. Lymph node metastasis is not rare in advanced HCC (*30*), but confirmation of metastases to lymph nodes smaller than 1 cm in diameter is not possible through an imaging study. Moreover, previous transarterial chemoembolization, hepatitis, endoscopic procedures on varices, and peritonitis, all

of which are common in HCC patients, can increase lymph node size. In our study, 3 of 5 index lesions of lymph nodes greater than 1 cm in diameter tested positive on both ^{18}F-FDG PET/CT and ^{11}C-acetate PET/CT (data not shown).

In summary, this study prospectively investigated the value of ^{18}F-FDG and ^{11}C-acetate PET/CT in the detection of primary and metastatic HCC. The addition of ^{11}C-acetate to ^{18}F-FDG PET/CT increases overall sensitivity in the detection of primary HCC but not of extrahepatic metastases. ^{18}F-FDG PET/CT and ^{11}C-acetate PET/CT have a low sensitivity in the detection of small primary HCCs, but ^{18}F-FDG PET/CT has a comparatively high sensitivity in the detection of extrahepatic metastases. These results suggest that ^{18}F-FDG PET/CT and ^{11}C-acetate PET/CT appear not to be useful for the detection of small primary HCC but that ^{18}F-FDG PET/CT may be useful for the screening of extrahepatic metastases of HCC.

ACKNOWLEDGMENTS

We thank Dr. Ho Young Lee for his kind support with the interpretation of PET/CT scans. This work was financially supported by grant 0640390-1 from the National Cancer Center, Korea.

REFERENCES

1. Bruix J, Sherman M. Management of hepatocellular carcinoma. *Hepatology.* 2005;42:1208–1236.
2. Jonas S, Bechstein WO, Steinmüller T, et al. Vascular invasion and histopathologic grading determine outcome after liver transplantation for hepatocellular carcinoma in cirrhosis. *Hepatology.* 2001;33:1080–1086.
3. Bruix J, Sherman M, Llovet JM, et al. Clinical management of hepatocellular carcinoma: conclusions of the Barcelona-2000 EASL conference. European Association for the Study of the Liver. *J Hepatol.* 2001;35:421–430.
4. Park JW, An M, Choi JI, et al. Accuracy of clinical criteria for the diagnosis of hepatocellular carcinoma without biopsy in a hepatitis B virus-endemic area. *J Cancer Res Clin Oncol.* 2007;133:937–943.
5. Beyer T, Townsend DW, Brun T, et al. A combined PET/CT scanner for clinical oncology. *J Nucl Med.* 2000;41:1369–1379.
6. Ho CL, Yu SC, Yeung DW. ^{11}C-acetate PET imaging in hepatocellular carcinoma and other liver masses. *J Nucl Med.* 2003;44:213–221.
7. Chen YK, Hsieh DS, Liao CS, et al. Utility of FDG-PET for investigating unexplained serum AFP elevation in patients with suspected hepatocellular carcinoma recurrence. *Anticancer Res.* 2005;25:4719–4725.
8. Sugiyama M, Sakahara H, Torizuka T, et al. ^{18}F-FDG PET in the detection of extrahepatic metastases from hepatocellular carcinoma. *J Gastroenterol.* 2004; 39:961–968.
9. Bohm B, Voth M, Geoghegan J, et al. Impact of positron emission tomography on strategy in liver resection for primary and secondary liver tumors. *J Cancer Res Clin Oncol.* 2004;130:266–272.
10. Oyama N, Akino H, Kanamaru H, et al. ^{11}C-acetate PET imaging of prostate cancer. *J Nucl Med.* 2002;43:181–186.
11. Ho CL, Chen S, Yeung DW, Cheng TK. Dual-tracer PET/CT imaging in evaluation of metastatic hepatocellular carcinoma. *J Nucl Med.* 2007;48:902–909.
12. Wudel LJ Jr, Delbeke D, Morris D, et al. The role of [^{18}F]fluorodeoxyglucose positron emission tomography imaging in the evaluation of hepatocellular carcinoma. *Am Surg.* 2003;69:117–124.
13. Park JW, for the Korean Liver Cancer Study Group and National Cancer Center. Practice guideline for diagnosis and treatment of hepatocellular carcinoma [in Korean]. *Korean J Hepatol.* 2004;10:88–98.
14. Party IW. Terminology of nodular hepatocellular lesions. *Hepatology.* 1995; 22:983–993.
15. Roeda D, Dolle F, Crouzel C. An improvement of ^{11}C acetate synthesis: nonradioactive contaminants by irradiation-induced species emanating from the ^{11}C carbon dioxide production target. *Appl Radiat Isot.* 2002;57:857–860.
16. Kim S, Chung JK, Kim BT, et al. Relationship between gastrointestinal F-18-fluorodeoxyglucose accumulation and gastrointestinal symptoms in whole-body PET. *Clin Positron Imaging.* 1999;2:273–279.
17. Nagaoka S, Itano S, Ishibashi M, et al. Value of fusing PET plus CT images in hepatocellular carcinoma and combined hepatocellular and cholangiocarcinoma patients with extrahepatic metastases: preliminary findings. *Liver Int.* 2006; 26:781–788.
18. Seo S, Hatano E, Higashi T, et al. Fluorine-18 fluorodeoxyglucose positron emission tomography predicts tumor differentiation, P-glycoprotein expression, and outcome after resection in hepatocellular carcinoma. *Clin Cancer Res.* 2007;13:427–433.
19. Shiomi S, Nishiguchi S, Ishizu H, et al. Usefulness of positron emission tomography with fluorine-18-fluorodeoxyglucose for predicting outcome in patients with hepatocellular carcinoma. *Am J Gastroenterol.* 2001;96:1877–1880.
20. Yang SH, Suh KS, Lee HW, et al. The role of ^{18}F-FDG-PET imaging for the selection of liver transplantation candidates among hepatocellular carcinoma patients. *Liver Transpl.* 2006;12:1655–1660.
21. Sun L, Wu H, Guan YS. Positron emission tomography/computer tomography: challenge to conventional imaging modalities in evaluating primary and metastatic liver malignancies. *World J Gastroenterol.* 2007;13:2775–2783.
22. Trojan J, Schroeder O, Raedle J, et al. Fluorine-18 FDG positron emission tomography for imaging of hepatocellular carcinoma. *Am J Gastroenterol.* 1999;94:3314–3319.
23. Khan MA, Combs CS, Brunt EM, et al. Positron emission tomography scanning in the evaluation of hepatocellular carcinoma. *J Hepatol.* 2000;32:792–797.
24. Iwata Y, Shiomi S, Sasaki N, et al. Clinical usefulness of positron emission tomography with fluorine-18-fluorodeoxyglucose in the diagnosis of liver tumors. *Ann Nucl Med.* 2000;14:121–126.
25. Verhoef C, Valkema R, de Man RA, Krenning EP, Yzermans JN. Fluorine-18 FDG imaging in hepatocellular carcinoma using positron coincidence detection and single photon emission computed tomography. *Liver.* 2002;22:51–56.
26. Shin JA, Park JW, An M, et al. Diagnostic accuracy of ^{18}F-FDG positron emission tomography for evaluation of hepatocellular carcinoma [in Korean]. *Korean J Hepatol.* 2006;12:546–552.
27. Park KW, Park JW, Choi JI, et al. Survival analysis of 904 patients with hepatocellular carcinoma in a hepatitis B virus-endemic area. *J Gastroenterol Hepatol.* 2008;23:467–473.
28. Hatano E, Ikai I, Higashi T, et al. Preoperative positron emission tomography with fluorine-18-fluorodeoxyglucose is predictive of prognosis in patients with hepatocellular carcinoma after resection. *World J Surg.* 2006;30:1736–1741.
29. Fujimoto R, Higashi T, Nakamoto Y, et al. Diagnostic accuracy of bone metastases detection in cancer patients: comparison between bone scintigraphy and whole-body FDG-PET. *Ann Nucl Med.* 2006;20:399–408.
30. Watanabe J, Nakashima O, Kojiro M. Clinicopathologic study on lymph node metastasis of hepatocellular carcinoma: a retrospective study of 660 consecutive autopsy cases. *Jpn J Clin Oncol.* 1994;24:37–41.